Calculation of the small-angle x-ray and neutron scattering from nonrandom (regular) fractals

Paul W. Schmidt and Xie Dacai*
Physics Department, University of Missouri, Columbia, Missouri 65211
(Received 9 July 1985)

The intensity of the small-angle x-ray or neutron scattering has been calculated for two nonrandom (regular) fractals: the Menger sponge and a related fractal, called the fractal jack (a form similar to the metal six-pointed object used in the American children's game). The scatterers are assumed to be systems of independently scattering, randomly oriented identical nonrandom fractals constructed from a material with uniform density. The scattered intensity $I(q)$ can be expressed as a function of qa, where $q=4\pi\lambda^{-1}\sin(\theta/2)$; λ is the scattered wavelength; θ is the scattering angle, and a is the edge of the cube which is the starting approximant to the fractal. The calculations show that $I(q)$ is a monotonically decreasing function on which maxima and minima are superimposed. For large qa the monotonic decay is proportional to q^{-D}, where D is the fractal dimension. The first maximum for $q>0$ is a single peak located at $q=q_1$. Groups of maxima are found at $q=3^k q_1$, where k is a positive integer greater than 1. The number of maxima within a group becomes greater as k increases. Numerical calculations of $I(q)$ provide no evidence that the maxima and minima are damped and die out as q becomes larger. Thus $I(q)$ for the two nonrandom fractals does not appear to approach the simple power-law scattering proportional to q^{-D} which is characteristic of the small-angle scattering from random fractals. The techniques developed to calculate $I(q)$ for the Menger sponge and the fractal jack can also be employed to find the small-angle scattering from other nonrandom (regular) fractals.

I. INTRODUCTION

Although discussions of the theory and properties of fractals[1] devote much attention to nonrandom (regular) fractals, such as the Koch curve[2] or the Menger sponge,[3] most calculations of the small-angle x-ray and neutron scattering from fractals have dealt with random fractals[4–7] or pores with fractal boundaries.[8–10] The only exception of which we are aware is the work of Kjems and Schofield,[10] who have outlined properties of the small-angle scattering from nonrandom one-dimensional fractals.

In order to compare the scattering from random fractals with that from a nonrandom fractal structure, we therefore have developed equations for the small-angle x-ray and neutron scattering from an assembly of identical, randomly oriented, independently scattering Menger sponges constructed from a material with uniform density. We have used these results in some numerical calculations of the intensity. Our work, which employs a technique which is similar to the method of Kjems and Schofield,[10] is, as far as we know, the first study of the scattering from three-dimensional nonrandom fractals.

Nonrandom fractals are generated from an initial configuration by a sequence of approximants. The zero-order approximant for the Menger sponge, for example, is a uniform-density cube with edge a. Our technique gives an expression for the intensity $I_n(q)$ for the nth approximant to a regular fractal, where

$$q=4\pi\lambda^{-1}\sin(\theta/2)\gg 1 ,$$

λ is the scattered wavelength, and θ is the scattering angle.

Our results for the first four approximants to the Menger sponge show that there are both similarities and differences in the scattering from random and nonrandom fractals. A characteristic feature of the small-angle scattering from random fractals is[6] that if a is a length with the magnitude of the overall dimension of the fractal, the scattered intensity $I(q)$ for $qa\gg 1$ is proportional to q^{-D}, where D is the fractal dimension[11] of the fractal. Since this power law is such an important property of the scattering from random fractals, we expected the intensity which we calculated for the Menger sponge to exhibit a similar behavior.

However, as we explain in Sec. IV, our numerical calculations indicate that the intensity $I_n(q)$ from the nth approximant to a Menger sponge does *not* appear to approach a power law. Instead, we find that

$$I_n(3q)=3^{-D}I_{n-1}(q)+L_{n-1}(q) .$$

An expression for $L_{n-1}(q)$ is given in Sec. IV. In an interval of q where the nth approximant adequately describes the scattering, $I_{n-1}(q)$ will be nearly as reliable an approximation as $I_n(q)$, so that $I_n(3q)$ would be essentially equal to $3^{-D}I_n(q)$ if $L_{n-1}(q)$ were negligible.

We call the condition $I_n(3q)=3^{-D}I_n(q)$ a generalized power law. Like an ordinary power law, the generalized power law is satisfied when $I_n(q)$ is proportional to q^{-D}. We say that the power law is generalized because we find that in $I_n(q)$ there are maxima and minima which are superimposed on a decay proportional to q^{-D}. If the first subsidiary maximum (i.e., the maximum for the smallest value of q not equal to zero) of $I_n(q)$ occurs for $q=q_1$, the generalized power law states that there will be maxima at $q=3^k q_1$, where k is a positive integer.

Instead of a single maximum at $q=3^k q_1$, however, we find that in the neighborhood of $q=3^k q_1$ approximately $3k$ maxima of varying amplitude are superimposed on the curve proportional to q^{-D}. We ascribe these multiple higher-order maxima to the fact that $L_{n-1}(q)$ is *not* negligible.

As we have mentioned, the Menger sponge can be constructed from a sequence of approximants, beginning with a uniform-density cube with edge a. This uniform cube is defined to be the zero-order approximant. To obtain the first approximant, the uniform cube which is the preceding approximant is divided into 27 smaller cubes, each with edge one-third that of the uniform cube. The cubes with edge $a/3$ in the center of each face and at the center of the initial cube are then removed, leaving 20 cubes. Succeeding approximants are obtained by performing an analogous operation in which each of the cubes making up the next-lowest approximant is divided into 27 cubes, after which the cubes at the center of each face and at the center of each cube of the latter approximant are removed. The fractal dimension D of the Menger sponge is equal[3] to $\log 20/\log 3 \cong 2.73\ldots$.

As we explain in Sec. III, by a method analogous to that which we employ to calculate the scattering from a Menger sponge, we can compute the scattered intensity from a related fractal, which, for want of a better name, we have called the fractal jack because it has a form similar to the metal six-pointed object used in the American children's game. This fractal is similar, though not identical, to a two-dimensional fractal discussed by Vicsek.[12] The first approximant to the fractal jack is obtained from a cube with uniform density and edge a by dividing this cube into 27 cubes with edge one-third that of the original cube and then removing all of the cubes with edge $a/3$ *except* those in the center of each face and at the center of the original cube. After this operation, seven cubes with edge $a/3$ remain. Higher-order approximants are generated by performing the same operation on the each of the cubes of preceding approximant. Since the fractal jack is generated by retaining 7 out of the 27 cubes produced when the cube edge is divided by 3 to form the next approximant, the fractal dimension D of the fractal jack will be equal[13,14] to $\log 7/\log 3 \cong 1.77\ldots$.

II. THE SMALL-ANGLE SCATTERING FROM A MENGER SPONGE

To calculate the intensity $I_n(q)$ for an assembly of N identical independently scattering, randomly oriented nth approximants to Menger sponges, we use the equation[15]

$$I_n(q)=I_{00}N(V_n)^2\langle[F_n(\mathbf{q})]^2\rangle , \tag{1}$$

where $q=|\mathbf{q}|=4\pi\lambda^{-1}\sin(\theta/2)$; the vector $\mathbf{q}$ is parallel to $\boldsymbol{\alpha}-\boldsymbol{\alpha}_0$, where $\boldsymbol{\alpha}$ and $\boldsymbol{\alpha}_0$ are unit vectors in the directions of the scattered and incident beams, respectively, the symbols $\langle\ \rangle$ denote an average over all orientations, I_{00} is a constant,

$$V_n=(\tfrac{20}{27})^n a^3$$

is the volume of the *filled* region of the nth approximant to the sponge, a is the length of the edge of the cube which is the zero-order approximant, and the structure factor $F_n(\mathbf{q})$ of the nth approximant is given by

$$F_n(\mathbf{q})=(1/V_n)\int_{V_n} e^{i(\mathbf{q}\cdot\mathbf{r})}dV . \tag{2}$$

In (2) the origin of the volume integration is taken to be at the center of the sponge and $\mathbf{r}$ is a vector from this origin to the volume element dV. The structure factor $F_n(\mathbf{q})$ is normalized so that $F_n(0)=1$. Thus, from Eq. (1),

$$I_n(0)=I_{00}N(V_n)^2\langle[F_n(0)]^2\rangle=I_{00}N(V_n)^2 .$$

The structure factor $F_1(\mathbf{q})$ for the first approximant can be calculated from (2) by dividing a uniform-density cube with edge a into 27 cubes with edge $a/3$ and removing the seven cubes at the center of the first approximant and at the centers of its six faces. The structure factor $F_1(\mathbf{q})$ which is obtained from (2) can be expressed as

$$F_1(\mathbf{q})=G_1(\mathbf{q})F_0(\mathbf{q}/3) . \tag{3}$$

In (3)

$$G_n(\mathbf{q})=\tfrac{1}{20}\sum_{j=-1}^{1}\sum_{k=-1}^{1}\sum_{l=-1}^{1}\omega_{jkl}e^{i(\mathbf{q}\cdot\mathbf{R}^n_{jkl})} , \tag{4}$$

n is a positive integer,

$$\omega_{jkl}=(1-\delta_{j0}\delta_{k0})(1-\delta_{k0}\delta_{l0})(1-\delta_{j0}\delta_{l0}) , \tag{5}$$

δ_{ij} is the Kronecker delta symbol, and

$$\mathbf{R}^1_{jkl}=(a/3)(j\mathbf{x}+k\mathbf{y}+l\mathbf{z}) \tag{6}$$

is the vector from the center of the zero-order cube to the center of one of the cubes with edge $a/3$ into which the zero-order approximant is divided to form the first approximant, and $\mathbf{x}$, $\mathbf{y}$, and $\mathbf{z}$ are unit vectors in the directions of the x, y, and z axes, respectively. In addition,

$$F_0(\mathbf{q})=\frac{1}{V_0}\int_{V_0} e^{i(\mathbf{q}\cdot\mathbf{r})}dV$$
$$=\frac{\sin[(\mathbf{q}\cdot\mathbf{x})(a/2)]}{(\mathbf{q}\cdot\mathbf{x})(a/2)}\,\frac{\sin[(\mathbf{q}\cdot\mathbf{y})(a/2)]}{(\mathbf{q}\cdot\mathbf{y})(a/2)}\,\frac{\sin[(\mathbf{q}\cdot\mathbf{z})(a/2)]}{(\mathbf{q}\cdot\mathbf{z})(a/2)}$$

is the structure factor for the zero-order approximant (i.e., for a uniform-density cube with edge a). The origin of the x, y, and z axes is chosen to be at the center of the zero-order approximant, and the axes are oriented so that each cube face is perpendicular to one of the axes.

The quantity ω_{jkl} in $G_1(\mathbf{q})$ in Eq. (5) is equal to zero when two or more of the indices j, k, and l are zero. This definition of ω_{jkl} ensures that the triple sum in Eq. (4) includes only the cubes with edge $a/3$ which form the first approximant.

The second approximant $F_2(\mathbf{q})$ is obtained from $F_0(\mathbf{q}/3)$ by performing the same operation on $F_0(\mathbf{q}/3)$ that was employed to obtain $F_1(\mathbf{q})$ from the structure factor $F_0(\mathbf{q})$ of the zero-order approximant. The result of this calculation can be written as

$$F_2(\mathbf{q})=G_1(\mathbf{q})G_2(\mathbf{q})F_0(\mathbf{q}/9) ,$$

since from the definition of $G_n(\mathbf{q})$,

$$G_n(\mathbf{q})=G_{n-1}(\mathbf{q}/3) .$$

By induction

$$F_n(\mathbf{q})=\prod_{i=1}^{n} G_i(q)F_0(\mathbf{q}/(3^n)) . \tag{7}$$

From (1) and (7) we obtain

$$I_n(\mathbf{q})=I_{00}N(V_n)^2\left\langle \left[\prod_{i=1}^{n}[G_i(\mathbf{q})]^2\right][F_0(\mathbf{q}/(3^n))]^2\right\rangle . \tag{8}$$

When $\mathbf{q}$ is small enough that $F_0(\mathbf{q}/(3^n))\simeq 1$,

$$\frac{I_n(\mathbf{q})}{I_n(0)}=\left\langle\prod_{i=1}^{n}[G_i(\mathbf{q})]^2\right\rangle . \tag{9}$$

By use of (4), (9) can be expressed as

$$\prod_{i=1}^{n}[G_i(\mathbf{q})]^2\simeq\sum_{j=-T_n}^{T_n}\sum_{k=-T_n}^{T_n}\sum_{l=-T_n}^{T_n}A_{jkl}^{n}\cos(\mathbf{q}\cdot\mathbf{R}_{jkl}^{n}) , \tag{10}$$

where

$$\mathbf{R}_{jkl}^{n}=3^{-(n-1)}\mathbf{R}_{jkl}^{1}$$

and

$$T_n=3^n-1 . \tag{11}$$

After the A_{jkl}^{1} in (10) have been evaluated from (4) when $n=1$, the other coefficients A_{jkl}^{n} in (10) for $n>1$ can be calculated from the A_{jkl}^{1} in Table I by use of the result that

$$\prod_{i=1}^{n+t}[G_i(\mathbf{q})]^2=\left[\prod_{i=1}^{n}[G_i(\mathbf{q})]^2\right]\left[\prod_{j=1}^{t}[G_j(\mathbf{q}/3^n)]^2\right] .$$

From this calculation we find that

$$A_{jkl}^{n+t}=\sum_{p=p_{\min}}^{p_{\max}}\sum_{r=r_{\min}}^{r_{\max}}\sum_{s=s_{\min}}^{s_{\max}}A_{prs}^{n}A_{j-3^t p,k-3^t r,l-3^t s}^{t} . \tag{12}$$

In (12)

$$\begin{aligned}
p_{\max}&=\text{Minint}\left[T_n,\frac{j+T_t}{3^t}\right],\quad p_{\min}=\text{Maxint}\left[-T_n,\frac{j-T_t}{3^t}\right],\\
r_{\max}&=\text{Minint}\left[T_n,\frac{k+T_t}{3^t}\right],\quad p_{\min}=\text{Maxint}\left[-T_n,\frac{k-T_t}{3^t}\right],\\
s_{\max}&=\text{Minint}\left[T_n,\frac{l+T_t}{3^t}\right],\quad s_{\min}=\text{Maxint}\left[-T_n,\frac{l-T_t}{3^t}\right],
\end{aligned} \tag{13}$$

and

$$\begin{aligned}
&\text{Maxint}(x,y)=x_{\text{int}}^{\max},\quad x>y\\
&\text{Maxint}(x,y)=y_{\text{int}}^{\max},\quad x<y\\
&\text{Minint}(x,y)=x_{\text{int}}^{\min},\quad x<y\\
&\text{Minint}(x,y)=y_{\text{int}}^{\min},\quad x>y .
\end{aligned} \tag{14}$$

The quantities $x_{\text{int}}^{\max}$ and $y_{\text{int}}^{\max}$ in (14) are, respectively, the largest integers not greater than x or y. Similarly, $x_{\text{int}}^{\min}$ and $y_{\text{int}}^{\min}$ are the smallest integers not less than x or y, respectively. The A_{jkl}^{n} can be shown to have the same value when any two indices are interchanged and also to be independent of the signs of the indices. All of the A_{jkl}^{1} therefore can be obtained from those listed in Table I.

The average over orientation can be calculated[16] for each term in (10) by use of a polar coordinate system in which the z axis is chosen to be in the direction of $\mathbf{R}_{jkl}^{n}$. Therefore, from (1) and (10),

TABLE I. Values of the A_{jkl}^{1}. For convenience, $400A_{jkl}^{1}$ has been tabulated, rather than A_{jkl}^{1} itself. The A_{jkl}^{1} can thus be obtained by dividing the numbers in the table by 400. Since the values of the A_{jkl}^{1} remain constant when the order or sign of the indices is changed, all the A_{jkl}^{1} can be found from those in the table.

j	k	l	$400A_{jkl}^{1}$
0	0	0	20
1	0	0	8
1	1	0	4
1	1	1	0
2	0	0	8
2	1	0	4
2	1	1	2
2	2	0	3
2	2	1	2
2	2	2	1

$$\frac{I_n(q)}{I_n(0)}=\sum_{j=-T_n}^{T_n}\sum_{k=-T_n}^{T_n}\sum_{l=-T_n}^{T_n}A_{jkl}^{n}\frac{\sin(q\rho_{jkl}^{n})}{q\rho_{jkl}^{n}} , \tag{15}$$

where

$$\rho_{jkl}^{n}=(j^2+k^2+l^2)^{1/2}(a/3^n) . \tag{16}$$

III. THE FRACTAL JACK

Since the nth approximant to the fractal jack is constructed by dividing each cube in the preceding approximant into cubes with edge $a/3^n$ and retaining only the cubes at the center of each face and at the center of the each cube with edge $a/3^{n-1}$, the structure factor $E_n(\mathbf{q})$ for the nth approximant to the fractal jack can be obtained simply by replacing $\omega_{jkl}/20$ by $(1-\omega_{jkl})/7$ in Eq. (4). [The factor $\frac{1}{20}$ is changed to $\frac{1}{7}$ in order to satisfy the normalization condition $E_n(0)=0$.] Then, by a procedure analogous to that employed to calculate $I_n(q)$ for the

Menger sponge, the scattered intensity $K_n(q)$ for the fractal jack can be expressed as

$$K_n(q)=I_{00}N(U_n)^2\langle[E_n(\mathbf{q})]^2\rangle\ , \tag{17}$$

where

$$U_n=(\tfrac{7}{27})^n a^3\ ,$$

$$E_1(\mathbf{q})=H_1(\mathbf{q})F_0(\mathbf{q})\ ,$$

and

$$H_n(\mathbf{q})=\tfrac{1}{7}\sum_{j=-1}^{1}\sum_{k=-1}^{1}\sum_{l=-1}^{1}(1-\omega_{jkl})e^{i(\mathbf{q}\cdot\mathbf{R}^n_{jkl})}\ , \tag{18}$$

where n is a positive integer and

$$E_n(\mathbf{q})=\left[\prod_{i=1}^{n}H_i(\mathbf{q})\right]F_0(\mathbf{q}/(3^n))\ . \tag{19}$$

Thus

$$K_n(q)=I_{00}N(U_n)^2\left\langle\left[\prod_{i=1}^{n}[H_i(\mathbf{q})]^2\right][F_0(\mathbf{q}/(3^n))]^2\right\rangle\ . \tag{20}$$

For q sufficiently small that $F_0(\mathbf{q}/(3^n))\cong 1$,

$$\frac{K_n(q)}{K_n(0)}=\left\langle\prod_{i=1}^{n}[H_i(q)]^2\right\rangle\ . \tag{21}$$

The average over orientation in (21) can be performed in the same way as for the Menger sponge, so that

$$\frac{K_n(q)}{K_n(0)}=\sum_{j=-T_n}^{T_n}\sum_{k=-T_n}^{T_n}\sum_{l=-T_n}^{T_n}B^n_{jkl}\frac{\sin(q\rho^n_{jkl})}{q\rho^n_{jkl}}\ , \tag{22}$$

where the T_n and the ρ^n_{jkl} are given by (11) and (16), respectively, and

$$B^{n+t}_{jkl}=\sum_{p=p_{\min}}^{p_{\max}}\sum_{r=r_{\min}}^{r_{\max}}\sum_{s=s_{\min}}^{s_{\max}}B^n_{prs}B^t_{j-3^t p,k-3^t r,l-3^t s}\ . \tag{23}$$

From the values of B^1_{jkl} in Table II, the B^n_{jkl} can be calculated from (23) for $n\geq 1$. The limits in (23) are given by (13) and (14).

TABLE II. Values of the B^1_{jkl}. For convenience, $49B^1_{jkl}$ has been tabulated, rather than B^1_{jkl} itself. The B^1_{jkl} thus can be obtained by dividing the numbers in the table by 49. Since the values of the B^1_{jkl} remain constant when the order or sign of the indices is changed, all the B^1_{jkl} can be found from those in the table.

j	k	l	$49B^1_{jkl}$
0	0	0	7
1	0	0	2
1	1	0	2
1	1	1	0
2	0	0	1
2	1	0	0
2	1	1	0
2	2	0	0
2	2	1	0
2	2	2	0

IV. RESULTS AND DISCUSSION

We have computed $I_n(q)/I_n(0)$ and $K_n(q)/K_n(0)$ from (15) and (22), respectively, for $2\leq n\leq 4$ and for $0<qa\leq 81$. (Copies of our FORTRAN programs are available.) Our results for $n=4$ are shown in Figs. 1 and 2. We have as yet been unable to extend our calculations to larger n for either the Menger sponge or the fractal jack because for $n>4$ our program uses more memory than is available on the University of Missouri's computer and also requires prohibitively long computing times.

As we have mentioned, (15) and (22) are valid only when the magnitude of q is small enough that

$$F_0(\mathbf{q}/(3^n))\cong 1\ .$$

This condition can be employed to estimate the value of

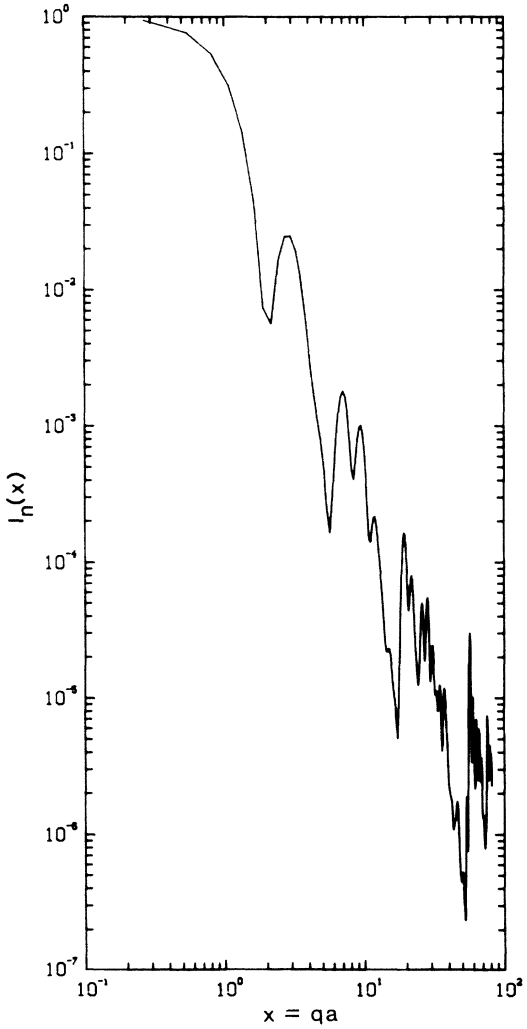

FIG. 1. Scattered intensity $I_n(x)$ for the Menger sponge calculated from (15) for $n=4$, plotted as a function of $x=qa$. As is mentioned in the text, the magnitude of $I_n(x)$ is somewhat too large for $x>50$, but the positions of the maxima and minima are nearly correct.

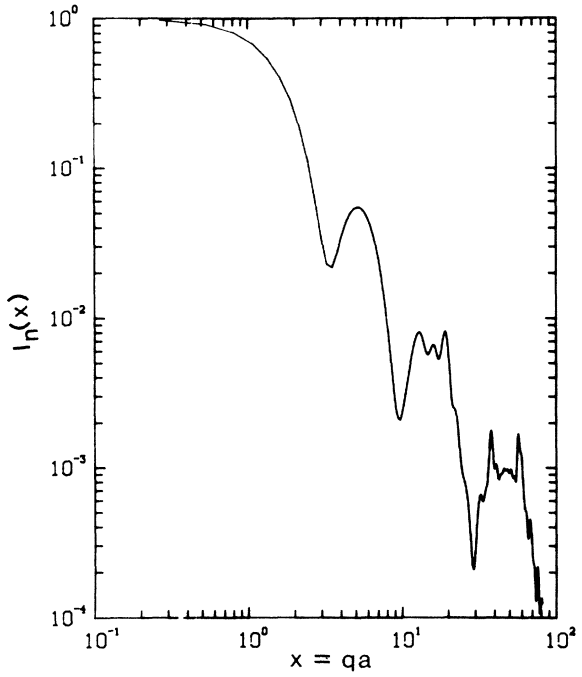

FIG. 2. Intensity $K_n(x)$ for the fractal jack calculated from (22) for $n=4$, plotted as a function of $x=qa$. The magnitude of $I_n(x)$ is somewhat too large for $x>50$, although the positions of the maxima and minima are nearly correct.

$x=qa$ for which (15) and (22) will give reliable intensities. From the definition of the structure factor $F_0(\mathbf{q})$ in Eq. (6), if $qa \ll 3^n$,

$$F_0(\mathbf{q}/(3^n)) \simeq 1 - \tfrac{1}{24}[qa/(3^n)]^2 . \tag{24}$$

To terms of order $(qa)^2$, the relative error resulting from the approximation $[F_0(q/(3^n))]^2 \simeq 1$ in (15) or (22) will therefore be

$$\tfrac{1}{12}[qa/(3^n)]^2$$

and thus will be less than 1% if $\frac{1}{12}[qa/(3^n)]^2 < 0.01$. As this condition will be satisfied when $x=qa < 0.1\sqrt{123}^n$, for the fourth approximant (i.e., for $n=4$), qa should not exceed 28. This result is consistent with our observation that within the accuracy of the lines on the plots in Figs. 1 and 2, the curves for the fourth approximant did not differ noticeably from those for the third approximant when x was less than 50. However, for 50×81, the intensities in Figs. 1 and 2 are too large. Our calculations for $n=3$ and $n=4$ suggest, on the other hand, that in a more precise calculation, the *positions* of the maxima and minima corresponding to those in Figs. 1 and 2 for $x>50$ are more reliable than the magnitudes of the intensities.

For random fractal aggregates with fractal dimension D, the scattered intensity for large qa is[6] proportional to q^{-D}. As can be seen from Figs. 1 and 2, however, for large x the scattering from the Menger sponge and the fractal jack does *not* follow the simple power law which is a characteristic of the scattering from random fractals. Instead, groups of maxima and minima are superimposed on a monotonically decreasing curve proportional to q^{-D}. Moreover, the pattern of maxima and minima within each group seems to become more complex as q increases, and our calculations do not suggest that the maxima and minima will be more highly damped as qa becomes larger. Although we cannot predict the properties of $I_n(q)$ and $K_n(q)$ for $n \gg 4$ from our numerical calculations for $n \leq 4$, we would like to emphasize that the intensities plotted in Figs. 1 and 2 give absolutely *no* indication that the scattering will *ever* approach a simple power law. The oscillations superimposed on the power-law decay of the scattered intensity which we have recently computed[17] for two one-dimensional nonrandom fractals also show no tendency to decay as q increases.

If the decay on which the oscillations are superimposed is proportional to q^{-D}, the product $q^D I_n(q)$ should be a function in which the amplitude of the oscillations is bounded. Plots of $q^D I_n(q)$ and $q^D K_n(q)$ for the Menger sponge and the fractal jack, respectively, are shown in Figs. 3 and 4. Since for $x<50$ the oscillations in these plots are bounded, the plots suggest that for both of these two nonrandom fractals the scattered intensity at large q is proportional to the product of q^{-D} and a function with oscillations which have a bounded amplitude.

We will now examine Eq. (9) in order to illustrate in more detail the conditions under which $I_n(q)$ will be proportional to the product of q^{-D} and a function which oscillates with a bounded amplitude. (Analogous results are true for the fractal jack.) From Eq. (4)

$$G_i(3\mathbf{q}) = G_{i-1}(\mathbf{q})$$

for $i>1$. Therefore, when $F_0[\mathbf{q}/(3^n)] \cong 1$, we find from (9) that

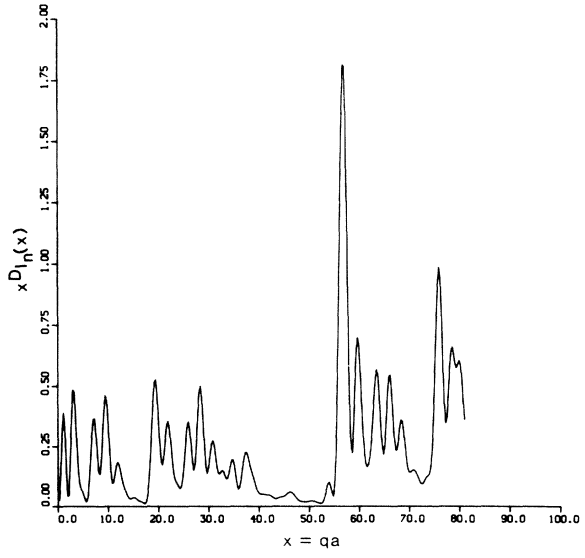

FIG. 3. Product $x^D I_n(x)$ for the Menger sponge for $n=4$ plotted as a function of $x=qa$. Even though for $x>50$ the magnitude of $x^D I_n(x)$ is somewhat too large, the positions of the maxima and minima are nearly correct.

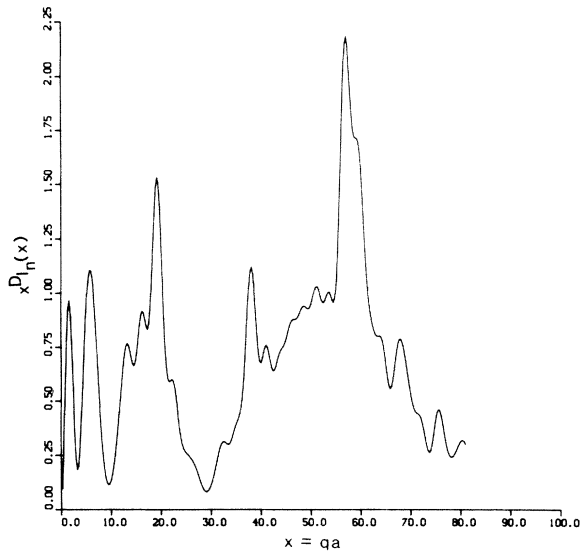

FIG. 4. Product $x^D K_n(x)$ for the fractal jack for $n=4$ plotted as a function of $x=qa$. While the magnitude of $x^D K_n(x)$ is somewhat too large for $x>50$, the positions of the maxima and minima are nearly correct.

$$\frac{I_n(3q)}{I_n(0)}=\left\langle\prod_{i=1}^{n}[G_i(3\mathbf{q})]^2\right\rangle$$
$$=\left\langle[G_1(3\mathbf{q})]^2\prod_{i=1}^{n-1}[G_i(\mathbf{q})]^2\right\rangle .$$

Thus, because

$$A^1_{000}=\frac{1}{20}=3^{-\log 20/\log 3} ,$$
$$\frac{I_n(3q)}{I_n(0)}=3^{-\log 20/\log 3}\frac{I_{n-1}(q)}{I_{n-1}(0)}+L_{n-1}(q) , \tag{25}$$

where

$$L_{n-1}(q)=\left\langle\{[G_1(3q)]^2-A^1_{000}\}\prod_{i=1}^{n-1}[G_i(q)]^2\right\rangle .$$

According to (25), if $L_{n-1}(q)$ were negligible, the equation

$$(3q)^D I_n(3q)=q^D I_n(q) \tag{26}$$

would be obtained. If (26) were satisfied, $I_n(q)$ could be written as

$$I_n(q)=q^{-D}g(q) ,$$

and the function $g_n(q)=q^D I_n(q)$ would have the property that[18]

$$g(3q)=g(q) .$$

When $g(q)$ is constant, the scattered intensity is proportional to q^{-D}, as is true for random fractals. When there are maxima and minima in $g(q)$, successive extrema are located at q values 3 times those of the preceding extremum, so that if the first nonzero value of q for which there is a maximum is q_1, there also are maxima at approximately $3^k q_1$, where k is a positive integer.

The curves in Figs. 1 and 2, however, show quite clearly that (26) does *not* describe $I_n(q)$ for large qa. Therefore, $L_{n-1}(q)$ *cannot* be neglected. We believe that $L_{n-1}(q)$ must be the source of the increasing complexity of successive groups of maxima in $I_n(q)$.

The approximate centers of these groups, however, are located at the positions where (26) predicts single maxima. In a group of maxima centered around $3^k q_1$ in Figs. 1 and 2, there are approximately k maxima.

Even if we have not been able to find an approximation for $L_{n-1}(q)$ or even to develop techniques for estimating its magnitude, the curves in Figs. 1–4 suggest that although it is large enough to split the maxima at $3^k q_1$ predicted by (26), $L_{n-1}(q)$ is too small to change the order of magnitude of $I_n(q)$ from the values given by (26).

For random fractals,[4–7] the small-angle scattering for large q is proportional to q^{-D}, while for pores with fractal boundary surfaces[8–10] it decays with q^{6-D}. Since the cubic cavities in the Menger sponge suggest that this fractal might be considered to be a model of a material with fractal pores, we were not sure whether the scattering for the Menger sponge would be more like that from a random fractal or from a material with fractal pores until we saw the results of our calculations of $I_n(q)$ and $K_n(q)$.

Figures 1 and 3, however, illustrate that the monotonic decay on which the maxima and minima are superimposed is proportional to q^{-D}, and not to $q^{-(6-D)}$. After thinking about this result, we realized that the intensity calculated from (15) cannot be considered to be the scattering from the cavities in the Menger sponge. Although the small-angle-scattering analogue of the Babinet principle[19] states that a system of pores in a material with uniform density will scatter like an assembly of uniform particles which have the same shape as the pores, this result is valid only when the overall dimensions of the system are so large that the effect on the scattering intensity resulting from these overall dimensions occurs at scattering angles too small to be observable. (A hollow sphere with outer radius a and inner radius b, for example, will scatter like a uniform sphere with radius b only if $a \gg b$ and also the scattering angles are so large that the outer radius a has no noticeable effect on the scattered intensity.) Our hindsight thus tells us that it really is not very surprising to find a decay proportional to q^{-D} for the scattering from the Menger sponge.

The results of our calculations lead us to suggest, though we have no rigorous proof, that both the splitting of the maxima and also the fact that these maxima do not appear to die out as q increases are the result of two competing symmetries which are present in the approximants to the Menger sponge and the fractal jack.[20] First, there is the cubic symmetry which is a result of the construction of the fractal by removing cubes from preceding approximants. This cubic symmetry and the resulting tendency to approach translational invariance produce intensity maxima analogous to Bragg reflections and probably are the cause of both the presence and the splitting of the subsidiary maxima. The second symmetry, which is the dilation invariance or self-similarity that is the defining characteristic of a fractal,[21] is the source of the decay pro-

portional to q^{-D} upon which the maxima and minima are superimposed.

The effects of these two symmetries, however, are not always easy to separate in the scattering curves. For example, because of the maxima and minima in the scattered intensity, the fractal dimension would not be easy to evaluate reliably from scattering curves like those in Figs. 1 and 2. This difficulty in extracting the fractal dimension for experimental data for nonrandom fractals may be related to the some of the problems Avnir *et al.*[22] encountered in their attempts to determine the fractal dimension of nonrandom fractals by image analysis.

In their calculations of the optical diffraction[23] and x-ray and neutron small-angle scattering[10] from some nonrandom fractals, Allain and Cloitre[23] and Kjems and Schofield[10] have employed methods similar to those which we have described.

The techniques which we have developed for computing the scattered intensity from the Menger sponge and the modified sponge can be easily modified to find the scattering from other nonrandom fractals. For nonrandom fractals constructed by dividing the preceding approximant into parts and removing some of these pieces, functions analogous to $G_n(\mathbf{q})$ and $F_0(\mathbf{q}/(3^n))$ can be obtained. The intensity $I_n(\mathbf{q})/I_n(0)$ for these fractals can then be calculated, and the error in approximating the structure factor by the expression $F_0(\mathbf{q})\simeq 1$ can be estimated.

ACKNOWLEDGMENTS

Acknowledgment is made to the Donors of the Petroleum Research Fund, administered by the American Chemical Society, for support of this work. We are extremely grateful for the help and advice which we received from Peter Pfeifer, who suggested our study of the scattering from the Menger sponge and who provided much assistance in the analysis and interpretation of our results. We also express our sincere appreciation to Ronald Lovett, David Avnir, Michael Bretz, Dann Passoja, and Fred Ross for their comments about our manuscript and the interpretation of our calculations and to T. W. Edwards, G. P. Aldredge, and W. L. Churchill for their assistance with the numerical calculations.

---

*Permanent address: Jiang-Xi Institute of Metallurgy, Gan-Zhou, People's Republic of China.

[1]B. B. Mandelbrot, *The Fractal Geometry of Nature* (Freeman, San Francisco, 1982).

[2]B. B. Mandelbrot, *The Fractal Geometry of Nature,* Ref. 1, Chap. 6.

[3](a) B. B. Mandelbrot, *The Fractal Geometry of Nature,* Ref. 1, pp. 134 and 145; (b) P. Pfeifer and D. Avnir, J. Chem. Phys. **79**, 3560 (1983).

[4]D. W. Schaefer and K. D. Keefer, Phys. Rev. Lett. **53**, 1283 (1984).

[5]D. W. Schaefer, J. E. Martin, D. Cannell, and P. Wiltzius, Phys. Rev. Lett. **52**, 2371 (1984).

[6]J. E. Martin and B. J. Ackerson, Phys. Rev. A **31**, 1180 (1985).

[7]S. K. Sinha, Y. Freltoft, and J. Kjems, in *Kinetics of Aggregation and Gelation,* edited by F. Family and D. P. Landau (North-Holland/Elsevier, Amsterdam, 1984), pp. 87–90.

[8]H. D. Bale and P. W. Schmidt, Phys. Rev. Lett. **53**, 596 (1984).

[9]J. Kjems, in Abstracts of Papers presented at the Symposium on Small-Angle Scattering and Related Methods, Hamburg, West Germany, 1984 (unpublished), p. 19.

[10]J. Kjems and P. Schofield, in *Scaling Phenomena in Disordered Systems,* NATO Advanced Studies Institute, Series B (Physics) edited by Pynn and Skjeltorp (Plenum, New York, in press).

[11]B. B. Mandelbrot, *The Fractal Geometry of Nature,* Ref. 1, p. 15, Chaps. 5 and 6.

[12]T. Vicsek, Proc. Phys. Soc. London Sect. A **16**, L647 (1983).

[13]P. Pfeifer and D. Avnir, J. Chem. Phys., Ref. 3(b), Eq. (1).

[14]B. B. Mandelbrot, *The Fractal Geometry of Nature,* Ref. 1, pp. 37 and 38.

[15]A. Guinier, G. Fournet, C. B. Walker, and K. L. Yudowitch, *Small-Angle Scattering of X-Rays* (Wiley, New York, 1955), pp. 5–8.

[16]A. Guinier, G. Fournet, C. B. Walker, and K. L. Yudowitch, *Small-Angle Scattering of X-Rays,* Ref. 15, Eq. (7), p. 8.

[17]M. Penk and P. W. Schmidt (unpublished).

[18]We are grateful to Peter Pfeifer for pointing out this result.

[19]A. Guinier, G. Fournet, C. B. Walker, and K. L. Yudowitch, *Small-Angle Scattering of X-Rays,* Ref. 15, pp. 38–40.

[20]We thank Peter Pfeifer for suggesting the presence of this competition.

[21]B. B. Mandelbrot, *The Fractal Geometry of Nature,* Ref. 1, pp. 34, 349, and 350.

[22]D. Farin, S. Peleg, D. Yavin, and D. Avnir, Langmuir **1**, 399 (1985), especially Sec. IV and Table III.

[23]C. Allain and M. Cloitre (unpublished); abstract in J. Stat. Phys. **39**, 247 (1985).